Monitoring Engineered Remediation with Borehole Radar

By John W. Lane, Jr., Frederick D. Day-Lewis, and Peter K. Joesten

U.S. Geological Survey, Office of Ground Water, Branch of Geophysics, 11 Sherman Place, Unit 5015, Storrs, CT 06269

Corresponding author:
John W. Lane, Jr.: email: *jwlane@usgs.gov*, ph: 860-487-7402 x13, fax: 860-487-8802

Final copy as submitted to The Leading Edge for publication as: Lane, J.W., Jr., Day-Lewis, F.D., and Joesten, P.K., 2007, Monitoring engineered remediation with borehole radar: The Leading Edge, v.26, no. 8, p. 1032-1035.

The success of engineered remediation is predicated on correct emplacement of either amendments (e.g., vegetable-oil emulsion, lactate, molasses, etc.) or permeable reactive barriers (e.g., vegetable oil, zero-valent iron, etc.) to enhance microbial breakdown of contaminants and treat contaminants. Currently, site managers have limited tools to provide information about (1) the distribution of injected materials; (2) the existence of gaps or holes in barriers; and (3) breakdown or transformation of injected materials over time. Current technologies for evaluating or confirming the success of emplacements primarily rely on direct measurements from wells. Such measurements are invasive, expensive, time consuming, and provide only limited spatial and temporal information. Given that microbial activity can be highly localized and conventional fluid sampling is sparse (in space and time), new approaches are required for cost-effective verification of engineered remediation. In this article, we discuss the application of borehole-radar techniques to monitor engineered remediation. We review the basis for cross-hole radar monitoring of remediation processes and provide two case studies. In the first study, borehole radar was used to evaluate the emplacement of vegetable oil emulsion in a pilot study to promote biodegradation of chlorinated solvents. In the second study, borehole radar was used to monitor the installation of a permeable reactive iron wall, again part of a pilot study to remediate chlorinated solvents. Our results demonstrate that radar data can provide information to (1) improve or extend the interpretation of conventional geochemical samples, and (2) optimize selection of locations for additional geochemical sampling or drilling.

Borehole radar: Principles and Data Acquisition

Surface and borehole radar methods use high-frequency (MHz to GHz) EM waves to investigate the earth. Cross-hole measurements of EM-wave traveltime and (or) amplitude provide information about subsurface lithology, structure, porosity, and pore fluids. The utility of

radar methods for time-lapse monitoring of injection experiments depends on the contrasts between the dielectric permittivity and (or) electrical conductivity of the injectate relative to those of the native pore fluid. The slowness (reciprocal velocity) at which radar-frequency EM waves propagate is a strong function of dielectric permittivity (Equation 1, Box 1).

Bulk dielectric permittivity depends on the soil or rock matrix, porosity, pore fluid, and saturation. The dielectric permittivity of several common amendments differs substantially from that of water. For example, the relative permittivity of vegetable oil, ε_r^{oil}, is about 2.9-3.5, whereas that of water, $\varepsilon_r^{H_2O}$, is about 80. Depending on the percent of oil, amendments of vegetable oil emulsion (VOE) can have strong radar signatures. The emplacement of VOE in saturated materials results in a decrease in radar slowness (increase radar propagation velocity), where changes in slowness are a linear function of the VOE saturation (Equation 2, Box 1).

The attenuation of radar-frequency EM waves is a strong function of electrical conductivity, which depends on the chemical composition of the soil or rock matrix and pore fluid. In low-loss, non-magnetic earth materials where EM waves propagate relatively independent of frequency, EM attenuation can be approximated as a simple function of the electrical conductivity and dielectric permittivity of the medium (Equation 3, Box 1). In the context of cross-hole radar monitoring, we assume temporal changes in attenuation relative to background measurements are caused by changes in pore fluid specific conductivity, which can be related to changes in total dissolved solids (TDS) by combining Equation 3 (Box 1) with Archie's Law and any of several relations used to convert between TDS and fluid specific conductivity.

Cross-hole radar data acquisition geometries suitable for monitoring range from the simple to complex. In the simplest configuration, zero-offset profiles (ZOPs), or gathers, can be used to rapidly scan the interwell region by moving the radar transmitter and receiver in small

increments along boreholes bounding the area of interest. Alternatively, multiple source and receiver gathers can be collected to allow for tomographic inversion (Figure 1).

Detection vs. Monitoring

Radar techniques have the potential, in principle, to detect many contaminants (e.g., chlorinated hydrocarbons) based on contrasts in dielectric permittivity and (or) electrical conductivity between the contaminants and water. In practice, however, detection has proven difficult, and the topic remains one of continued research. Detection is problematic because natural spatial variability in permittivity and conductivity can be large compared to the contrasts arising from different pore fluids (e.g., TCE vs. water). In research studies, where injections are controlled, it is possible to use difference inversion or processing to subtract out unchanged geologic variability, and reveal areas of time-lapse changes. In practice, this is seldom possible as background geophysical datasets are not collected prior to contaminant release.

Detection is a difficult problem at best. We draw a distinction, however, between the problem of *detection* and the far more tractable problem of *monitoring* by difference imaging. In the case of monitoring controlled, planned fluid injections, we can capitalize on the value of background data. The benefits of background data are illustrated with a simple numerical example for straight-ray tomography in Figure 2. Transmitter and receiver locations are assumed at 0.5-m intervals along boreholes on the left and right sides of the cross section. Given a background dataset and data collected after injection of an amendment, the use of difference tomography makes it possible to see the target material (Figure 2f), even in the presence of strong geologic variability (Figure 2a).

Another advantage in monitoring engineered remediation, as compared to detecting contaminants, is the opportunity to engineer or “dope” injectate. In cases where amendments

have weak electrical and (or) dielectric signatures (e.g., low mixture percentage or concentration), it may be possible to add tracers, such as colloidal iron, dissolved magnetite, or ionic solutions to enhance the radar signatures of amendments.

Case Study 1: Biostimulation with Vegetable Oil Emulsion

The U.S. Geological Survey used cross-hole radar to monitor a field-scale biostimulation pilot project conducted by the U.S. Navy at the Anoka County Riverfront Park (ACP), downgradient of the Naval Industrial Reserve Ordnance Plant, in Fridley, Minnesota. ZOP and full tomography surveys collected periodically from November 2001 to June 2003 were designed to (1) image the emplacement of about 14 m^3 of VOE (containing about 1/3 vegetable oil and 2/3 water) and (2) monitor possible VOE movement and changes in downgradient water chemistry resulting from VOE dissolution and (or) enhanced microbial activity. The presence of VOE in the saturated zone was expected to initially decrease radar attenuation because of the lower electrical conductivity of VOE relative to that of native ground water. Over time, the electrical conductivity of ground water in contact with or downgradient of the VOE plume may increase because of microbial activity and other geochemical and biodegradation processes that break down the VOE and contaminants and reduce solid mineral species to aqueous form.

Radar data were collected using a single-channel Malå GeoScience RAMAC[1] borehole radar system and broad-band electric dipole antennas (Figure 3) with center frequencies in air of about 100 MHz and therefore a dominant wavelength in the subsurface of about 0.75 m. A dense network of wells (13 boreholes in a 20-m by 20-m area) enabled high-resolution mapping of VOE using a combination of ZOP and tomography. Due to the speed of ZOP data collection,

[1] The use of trade, product, or firm names is for descriptive purposes only and does not imply endorsement by the U.S. Government.

ZOP scanning was conducted over much of the field site, whereas more time-intensive tomography surveys were limited to boreholes near the injection zone.

First-arrival times of both ZOP and tomography data were analyzed to estimate radar slowness changes. Amplitude analysis was performed only on ZOP data to calculate attenuation changes. Figure 4 shows example data for one borehole pair including an injection borehole (INJ-3). During the study period, changes in radar slowness expected for regions containing VOE were limited to boreholes straddling the injection zone (Figure 4a). No significant slowness changes were observed in downgradient ZOP scans (not shown); hence the geophysical results suggest the VOE remained proximal to the injection wells subsequent to emplacement. Tomograms (Figure 4c) corroborate the ZOP results and further suggest that injected amendments remain within several meters of the injection zones.

In contrast, radar amplitudes decreased significantly over the study period (Figure 4b) in boreholes within and downgradient of the injection zone, indicating increases in pore-fluid specific conductance; this is consistent with dissolution of the VOE and (or) biological activity. In many cases, changes in attenuation are observed for locations where either (1) no observation wells are located, or (2) observation wells are unscreened. The geophysical results thus provided valuable information about the spatial and temporal distributions of amendments and water-chemistry changes where fluid sampling was not possible; this information could be used to guide or optimize additional drilling and fluid-sampling.

Case Study 2: Installation of a Permeable Reactive Iron Wall

A pilot-scale study was conducted by the U.S. Army National Guard at the Massachusetts Military Reservation (MMR) on Cape Cod, Massachusetts, to evaluate the use of hydraulic fracturing of saturated sediments for installation of vertical, permeable reactive walls of zero-

valent iron (ZVI) to passively remediate chlorinated solvents. The study was conducted near the source area of the Chemical Spill-10 (CS-10). The U.S. Geological Survey conducted ZOP surveys across two iron walls (i.e., the "A-wall" and "B-wall") to evaluate the vertical and lateral extent of installations. A Malå GeoScience RAMAC borehole radar system and electric-dipole antennas with dominant center frequencies of 100 and 250 MHz were used. Because iron is highly conductive compared to native materials, the presence of iron should manifest as an increase in radar attenuation, and thus a decrease in amplitude.

A total of 23 cross-sections were scanned using borehole-radar ZOP, with 12 ZOPs crossing the A-wall and 13 crossing the B-wall. Because of damage to several key pre-injection monitoring boreholes, direct difference comparison was not possible for this study, and an alternative interpretation method was developed. After band-pass filtering, the maximum peak-to-peak amplitudes of direct waves were measured for each waveform trace. Amplitudes were normalized by the average amplitude observed in traces below the zone affected by injections, and interpolated to cross-sections co-located with the two iron walls (Figure 5). Interpretation of experimental results was guided by results from two-dimensional finite-difference time-domain (FDTD) modeling of EM wave propagation for iron walls (Figure 6). The FDTD model was used to identify a cutoff of normalized amplitude below which the presence of iron is indicated. A cutoff value of 0.43 was identified, and this was further verified with laboratory-scale physical modeling. Thus, regions of normalized amplitude (Figure 5) of less than this value are interpreted as iron wall. The FDTD model also was used to determine the potential of ZOP to resolve holes in the iron wall. Simulations suggest that holes with diameter less than 40% of the dominant wavelength will not be detected.

Our interpretation of field-experimental results suggests that (1) the hydraulic fracturing method successfully introduced iron into the subsurface; (2) the iron within the treatment zone is

distributed in a generally continuous manner; and (3) with the exception of a known gap in the A-wall, any holes present in the iron walls are smaller than the resolution limit of the radar.

Summary

Engineered remediation offers potentially cost-effective alternatives to traditional pump-and-treat remediation, but new approaches are needed to verify the emplacement of injected amendments and barriers and to confirm their effectiveness. Conventional fluid samples tend to be sparse—in both space and time—and offer limited information between observation wells. Cross-hole geophysical approaches have potential to address these problems, complement conventional sampling methods, and help design sampling strategies. Borehole radar, in particular, is highly sensitive to certain materials (e.g., vegetable-oil emulsion and zero-valent iron) commonly used for biostimulation and permeable reactive barriers. Studies presented here relied heavily on zero-offset profile data, which proved more practical and cost-effective to collect and process compared to more time-consuming tomography. Cross-hole radar results gave insights that would not have been possible given only conventional measurements at boreholes.

Acknowledgments

This work was supported by the U.S. Geological Survey Toxic Substances Hydrology Program. Funding for the two case studies was provided, in part, by U.S. Naval Facilities Engineering Command, Southern Division under MIPRs N6246701MP01929 and N6246702MP02932 (for work at the ACP); and by the Air Force Center for Environmental Excellence at the Massachusetts Military Reservation and the Army National Guard (for work at the MMR). The authors are grateful to Carole Johnson (USGS) for reviewing the manuscript.

Suggested Reading

Atekwana, E.A., Werkema, D.D., Jr., Duris, J.W., Rossbach, S, Atekwana, E.A., Sauck, W.A., Cassidy, D.P., Means, J., and Legall, F.D, 2004, In-situ apparent conductivity measurements and microbial population distribution at a hydrocarbon-contaminated site: Geophysics, 69, no. 1, p. 55-63.

Lane, John W., Jr., Joesten, Peter K., and Savoie, Jennifer G., 2001, Cross-Hole Radar Scanning of Two Vertical, Permeable, Reactive-Iron Walls at the Massachusetts Military Reservation, Cape Cod, Massachusetts: U.S. Geological Survey Water-Resources Investigations Report 00-4145, 17 p.

Lane, J.W., Jr., F.D. Day-Lewis, and C.C. Casey, 2006, Geophysical Monitoring of Field-Scale Vegetable Oil Injections for Biostimulation, *Ground Water*, doi: 10.1111/j.1745-6584.2005.00134.x, 14p.

Lane, J. W., Jr., Day-Lewis, F.D., Versteeg, R.J., and Casey, C.C., 2004, Object-based inversion of cross-well radar tomography to monitor injection experiments: Journal of Environmental and Engineering Geophysics, 9, no. 2, p. 63-77.

Ramirez, A.L., and Lytle, R.J., 1986, Investigation of fracture flow paths using alterant geophysical tomography: J. Rock Mech Min. Sci. Geomech. (International Journal of Rock Mechanics and Mining Sciences and Geomechanics Abstracts), **23**, p. 165-169.

Singha, K., Lane, J.W. Jr., and Kimball, K. (2000). Use of borehole-radar methods to characterize bedrock fractures and lithologic variations. U.S. Geological Survey Fact Sheet 054-00, 4p.

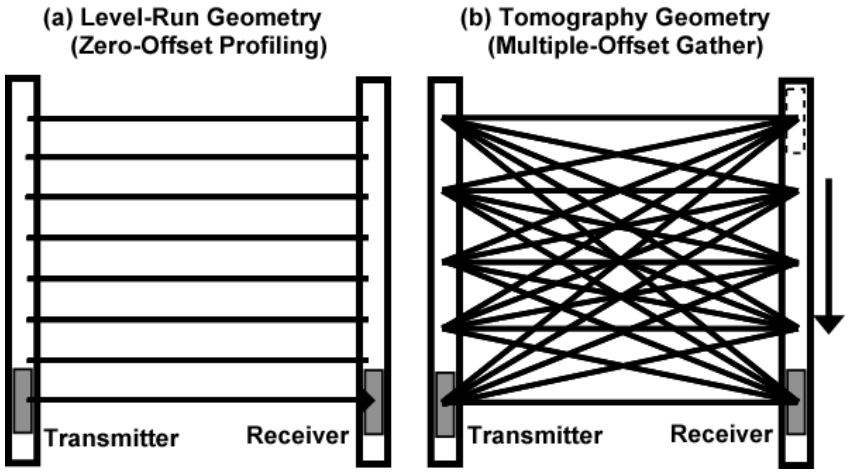

Figure 1. Radar survey geometries for (a) crosshole zero-offset profile (ZOP) and (b) crosshole tomography (Lane et al., 2006).

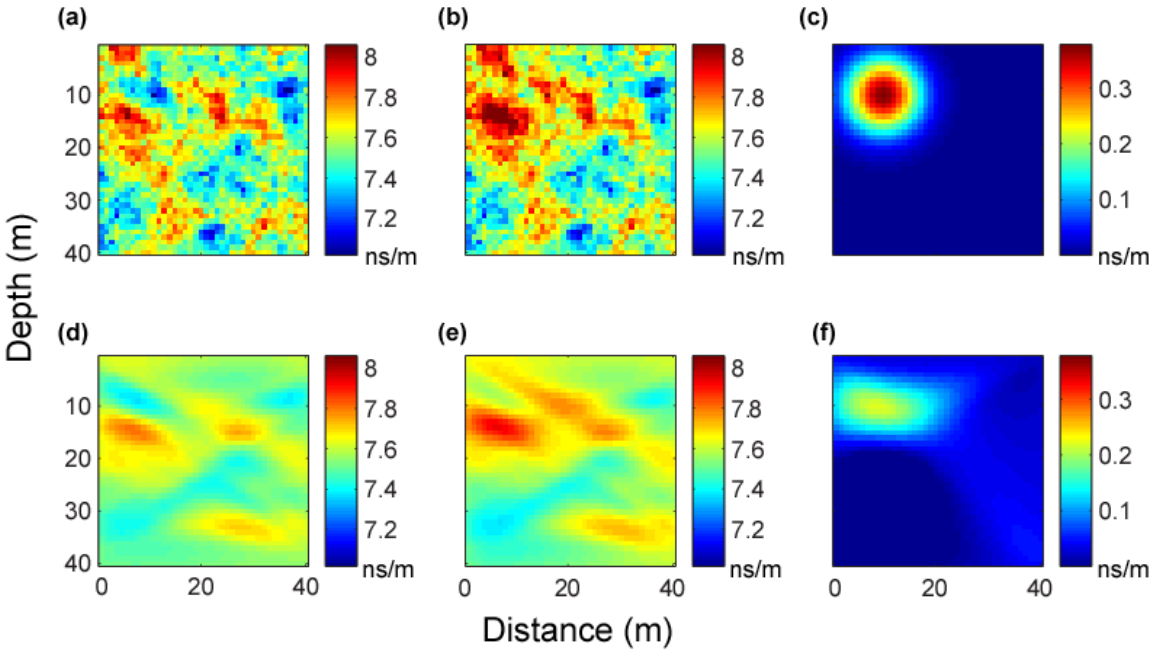

Figure 2. Numerical example illustrating the value of background data for slowness difference tomography. (a) Preinjection slowness, (b) postinjection slowness, and (c) the slowness difference associated with a hypothetical amendment target. (d) The tomogram based on preinjection data, (e) the tomogram based on postinjection data, and (f) the tomogram inverted from difference data. Given just postinjection data and (e), it would be extremely difficult to characterize the target plume; however, difference tomography (f) successfully reveals the target.

Figure 3. Photograph showing a 250-MHz borehole-radar antenna at the Massachusetts Military Reservation, Cape Cod, Massachusetts.

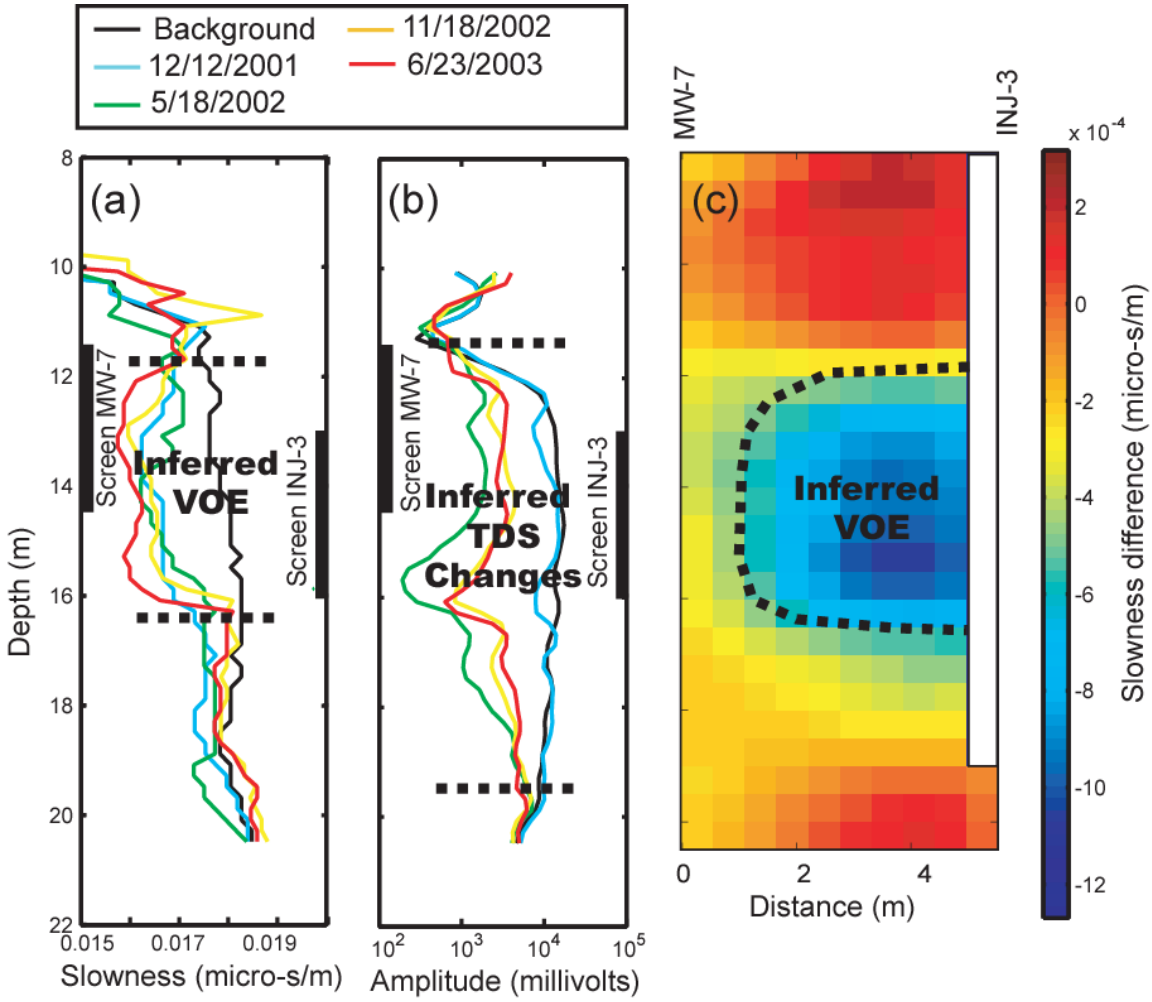

Figure 4. Field study. (a) Slowness zero-offset profile; (b) amplitude zero-offset profile; and (c) difference-slowness tomogram for the MW-7 to INJ-3 plane, Anoka County Riverfront Park, Fridley, Minnesota (Lane et al., 2006).

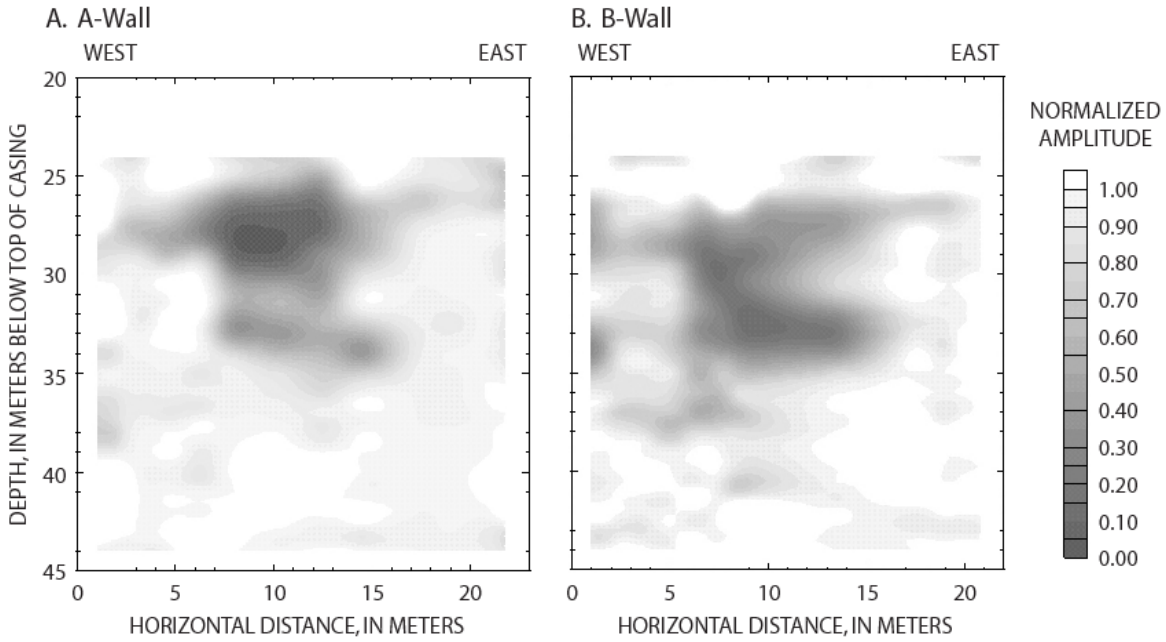

Figure 5. Postinjection direct-wave amplitudes across (a) A-wall, and (b) B-wall, Massachusetts Military Reservation (Lane et al., 2001).

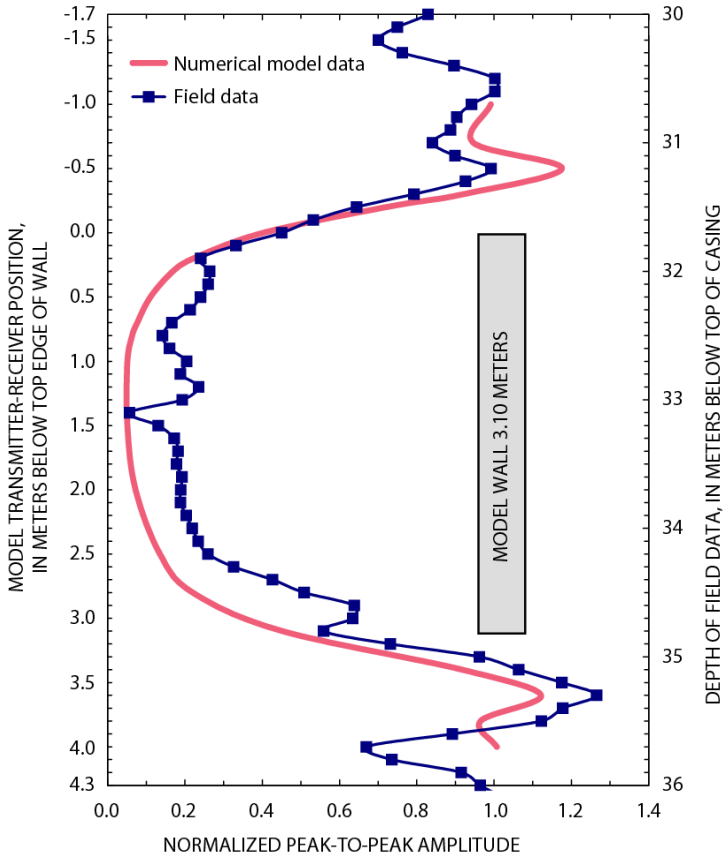

Figure 6. Simulated normalized model-wall amplitudes for a 3.10-m wall and the observed normalized field-data amplitudes from the zero-offset profile radar survey between boreholes RW-20 and RW-13, Massachusetts Military Reservation (Lane et al., 2001).

Box 1. Relations between electromagnetic properties and amendments.

Radar slowness (reciprocal velocity) can be approximated by

$$s = \frac{1}{v} \approx \frac{\sqrt{\varepsilon_r}}{c} \tag{1}$$

where,

s is radar slowness, in seconds/meter;
v is radar velocity, in meters/second;
c is the velocity of electromagnetic waves in a vacuum, in meters/second; and
ε_r is the dielectric permittivity of the medium, relative to a vacuum, dimensionless.

The saturation of vegetable-oil emulsion and difference slowness are linearly related by

$$S^{VOE} = \frac{-\Delta s \; c}{\phi\left(\sqrt{\varepsilon_r^{H_2O}} - \sqrt{\varepsilon_r^{VOE}}\right)}. \tag{2}$$

where,

S^{VOE} is the pore-space saturation of vegetable oil emulsion, dimensionless;
Δs is the difference in slowness from the background, pre-injection condition, in seconds/meter;
ϕ is the porosity, dimensionless;

ε_r^{VOE} is the relative dielectric permittivity of the VOE, dimensionless; and
$\varepsilon_r^{H_2O}$ is the relative dielectric permittivity of water, dimensionless.

In low-loss non-magnetic earth materials, radar attenuation can be approximated by

$$\alpha \approx B\sigma \,/\, \sqrt{\varepsilon_r} \tag{3}$$

where,

α is attenuation, in decibels/meter;
B is 1.68 x 103 dB/S; B incorporates free-space impedence and unit conversion from nepers to decibels; and
σ is the bulk electrical conductivity, in Siemens/meter.